International Journal of Computational and Experimental Science and ENgineering (IJCESEN)

Vol. 12-No.2 (2026) pp. 679-688
http://www.ijcesen.com

ISSN: 2149-9144

Research Article

High-Fat Diet Rapidly triggers Lipotoxicity, Hippocampal Neuroinflammation, CA1 Astrogliosis and Neuronal Injury in Rats.

M'hammed Amine Khene[1*], Ouarda Belabbassi[2], Kahina Chabane[3], Lokman Kechkoul[4], Mohamed El Fadel Ousmaal[5], Faiza Zaida[6], Djamila Benaziza[7]

[1] University of Ghardaïa, Faculty of Natural Sciences, Life and Earth Sciences, Department of Biology, 47000, Ghardaïa Algeria
* **Corresponding Author Email:** amine.khene@univ-ghardaia.edu.dz - **ORCID:** 0000-0001-7998-8071

[2] University of Ghardaïa, Faculty of Natural Sciences, Life and Earth Sciences, Department of Biology, 47000, Ghardaïa Algeria
Email: o.belabbassi@gmail.com - **ORCID:** 0000-0002-3690-3450

[3] USTHB-Bab Ezzouar, Faculty of Biological Sciences, 16111, Algiers-Algeria
Email: kahinachabane@hotmail.fr - **ORCID:** 0000-0002-7378-5449

[4]USTHB-Bab Ezzouar, Faculty of Biological Sciences, 16111, Algiers-Algeria
Email: fkajokerman@yahoo.com - **ORCID:** 0009-0008-6451-8073

[5] University of Algiers, Department of Natural and Life Sciences, Faculty of Sciences, 16000, Algiers-Algeria
Email: m.ousmaal@univ-alger.dz - **ORCID:** 0000-0002-6674-2782

[6] ENS- Kouba, Department of Biology, Laboratory of Biology and Animal physiology, 16308, Algiers-Algeria
Email: faiza.zaida@g.ens-kouba.dz - ORCID: 0009-0006-9938-8798

[7] ENS- Kouba, Department of Biology, Laboratory of Biology and Animal physiology, 16308, Algiers-Algeria
Email: djamila.benaziza@g.ens-kouba.dz - **ORCID**: 0000-0002-3878-5793

Article Info:

DOI: 10.22399/ijcesen.5294
Received: 10 December 2025
Revised: 24 March 2026
Accepted: 14 May 2026

Keywords

High-fat diet
Hippocampus
Oxidative stress
Astrogliosis
Spatial memory
CA1

Abstract:

While diet-induced obesity is firmly associated with cognitive decline, the early mechanisms linking peripheral metabolic dysfunction to central neurotoxicity remain poorly defined. This study investigated the rapid impact of systemic lipotoxicity on hippocampal functional and structural integrity. Male Wistar rats were administered either a standard diet or a high-fat diet (HFD) lipid emulsion for ten weeks. We evaluated systemic metabolic profiles, spatial working memory via the Y-maze, hippocampal transaminase activity, oxidative stress markers, neuroinflammation (IL-6), and structural alterations in the CA1 (Cornu Ammonis 1) subfield using Nissl and GFAP (Glial Fibrillary Acidic Protein) staining. The results showed that HFD intervention induced systemic dyslipidemia without altering fasting glucose or insulin levels. Behaviorally, HFD rats demonstrated significant spatial memory deficits. Biochemically, peripheral lipid overload prompted central metabolic distress, characterized by elevated hippocampal transaminase (ALT/AST) activity, a failure of endogenous antioxidant defenses, doubled lipid peroxidation, and a significant increase in pro-inflammatory IL-6 (Interleukine-6). Histologically, these biochemical disruptions translated into marked neuronal distress and widespread reactive astrogliosis within the CA1 pyramidal layer. Our findings revealed that the HFD consumption impairs spatial memory through a strictly lipotoxic mechanism, prior to the onset of overt hyperglycemia. Early systemic dyslipidemia severely disrupts central metabolic homeostasis, driving oxidative stress, neuroinflammation, Astrogliosis and consequent CA1 neuronal injury.

1. Introduction

With the worldwide adoption of the Western dietary pattern of chronic overconsumption of saturated fats and refined carbohydrates, diet-induced obesity has

become a major driver of systemic metabolic disease. In addition to the well-characterized cardiovascular and endocrine impact, a high-fat diet (HFD) exerts a profound impact on the central nervous system (CNS). Recent epidemiological and experimental evidence suggests a strong association between long-term high dietary lipid intake and early cognitive decline, as well as an increased risk of neurodegenerative diseases [1,2]. Specifically, systemic metabolic disturbances affect brain homeostasis well before clinical pathologies become overt and there is a need for a better understanding of the early mechanisms linking peripheral metabolic dysfunction and central neurotoxicity.

The hippocampus, a limbic structure important for memory consolidation and spatial navigation, is uniquely susceptible to dietary insults. The hippocampus is particularly vulnerable to oxidative damage and lipid-induced metabolic stress due to its very high oxygen consumption and matrix rich in polyunsaturated fatty acids [3,4]. Systemic dyslipidemia during HFD intake compromises the integrity of the blood-brain barrier (BBB). The subsequent invasion of circulating lipid perturbagens into brain parenchyma triggers a state of central lipotoxicity [5]. The lipid overload overwhelms the capacity of the local mitochondria and induces the overproduction of reactive oxygen species (ROS) and depletion of the endogenous antioxidant defense systems, leading to severe oxidative stress.

Crucially this biochemical distress is not happening in a vacuum. Oxidative damage synergizes with neuroinflammatory pathways and is largely mediated by activation of resident glial cells [6,7]. Lipid and ROS accumulation induce a phenotypic transition of astrocytes, which regulate synaptic glutamate uptake and metabolic support, into a hypertrophic reactive state called reactive astrogliosis [8,9]. This gliosis is associated with increased release of pro-inflammatory cytokines, such as interleukin-6 (IL-6), which further destabilizes the neuronal microenvironment, driving excitotoxicity and structural neurodegeneration [10,11]. The pyramidal subfield Cornu Ammonis 1 (CA1) of the hippocampus is especially vulnerable to these lipotoxic and inflammatory cascades and often shows structural damage that is associated with spatial memory deficits [12,13]. The association between obesogenic diets and cognitive impairment has been well established, but many experimental models utilize long-term (12–16 week) solid pellet feeding regimens. These long protocols often lead to frank glucotoxicity and advanced insulin resistance, which mask the capacity to isolate the specific early-phase effects of systemic lipotoxicity on the brain [5,14,15]. Moreover, transaminases (ALT: alanine aminotransferase and AST: Aspartate aminotransferase), are commonly used as hepatic markers of lipid stress, but their potential as early markers of mitochondrial and metabolic distress in the malate-aspartate shuttle of the brain has not been sufficiently explored in short-term dietary interventions [16,17,18].

To fill these gaps the present study applied a carefully controlled lipid emulsion-based delivery system for 10 weeks in male Wistar rats. The model was designed to induce rapid and uniform systemic dyslipidemia, without the immediate development of overt hyperglycemia. The main goal was to examine the early time course of peripheral lipotoxicity-induced hippocampal oxidative stress, increased local transaminase activity and reactive astrogliosis. We also sought to determine how these biochemical and inflammatory changes translate into structural histopathological damage in the highly vulnerable CA1 subfield resulting in the impairment of hippocampus-dependent spatial working memory.

2. Material and Methods

2.1. Animals and conditions of housing

The study was conducted on twenty-four adult male Wistar rats (250–300 g, 8–10 weeks old) from Pasteur Institute of Kouba (Algiers, Algeria) to assess the physiological and neurological effects of dietary lipid overload. Upon arrival, the animals were placed in standard polypropylene cages under strictly controlled environmental conditions including a stable ambient temperature (24 ± 2°C), relative humidity of 40–60% and a standard 12-hour light/dark cycle. Animals had free access to standard rodent chow and tap water. The experimental protocols and animal care procedures were strictly performed in accordance with institutional and international guidelines for the care and use of laboratory animals and were formally approved by the Local Ethics Committee.

2.2. Dietary Intervention and Experimental Design

Following a two-week acclimatization period to minimize baseline stress, the rats were randomly assigned to either a control group (CON, n = 12) or a high-fat diet group (HFD, n = 12). The dietary intervention was maintained for ten consecutive weeks to establish a robust systemic and central metabolic phenotype.The control group was maintained on standard laboratory normal diet (ND) pellets (49.15% carbohydrates, 25.50% protein, 7.00% fat; SARL Production Locale, Bouzaréah, Algeria). The ND rats were given equal volumes of

saline and Tween-80 via gavage daily. To rapidly and uniformly induce systemic dyslipidemia and subsequent neuroinflammation overcoming the variability often seen in pellet-based HFD models, the HFD group received the standard diet supplemented with a highly concentrated lipid emulsion. This daily high-fat emulsion (1 mL/rat) was administered via oral gavage every morning. The emulsion formula was carefully standardized to consist of corn oil (150 g), milk powder (20 g), cholesterol (15 g), sucrose (15 g), sodium deoxycholate (1 g), cooking salt (5 g), Tween-80 (10 g), and distilled water (100 mL), enriched with a standard vitamin and mineral mixture. The mixture was stored at 4°C and thoroughly homogenized in a 41°C water bath immediately prior to administration to ensure consistent lipid delivery.

To evaluate the somatic effect of the dietary intervention, body weights were recorded at baseline (initial body weight, IBW) and at the end of the 10-week period (final body weight, FBW). Percentage weight gain was calculated as:

$$\text{weight gain (\%)} = [(FBW - IBW) / IBW] \times 100.$$

2.3. Y-Maze Spontaneous Alternation Test

The Y-maze spontaneous alternation test was conducted on day 71 (24 hours after the last gavage). This hippocampal-dependent task depends on the natural tendency of rodents to explore novel environments rather than to revisit previously explored ones [19,20].

The apparatus was made of opaque polyvinyl chloride (PVC) to remove extramaze visual cues. The apparatus was composed of three identical arms (65 cm length × 15 cm width × 31 cm height) arranged at 120° angles radiating from a central point. Testing was conducted in an isolated quiet room with uniform light (200 lux) between 10:00 and 11:00 a.m. Each rat was placed at the remote end of a given starting arm and allowed to explore the maze freely for 5 min. The observations were made using cameras in a separate room to avoid any interference, to record the order of the arms entries. An alternation was defined strictly as entering all three different arms consecutively (e.g. ABC, BCA, CAB). The apparatus was thoroughly cleaned with 5% ethanol between trials to remove olfactory traces. Spatial working memory was calculated as follows:

Alternation (%) = (Number of alternations / Total arm entries − 2) × 100.

2.4. Blood Collection and Systemic Metabolic Profiling

On day 72 rats were fasted overnight for 12 hours to establish the peripheral metabolic basis prior to central neurotoxicity. Animals were anesthetized by intraperitoneal injection of ketamine hydrochloride at 150 mg/kg body weight. Once deep surgical anaesthesia was confirmed (absence of pedal withdrawal reflex), blood was immediately collected by cardiac puncture from the left ventricle into heparinized tubes. Samples were centrifuged at 1,500 × g for 15 min at room temperature. The extracted serum was carefully removed, aliquoted into Eppendorf tubes and stored at −40°C for downstream biochemical profiling.

Fasting blood glucose was measured directly with a commercial glucometer (ACCU-CHEK Active; Roche Diagnostics, Mannheim, Germany). Serum insulin was measured by Chemiluminescence Immunoassay MAGLUMI™800 (New Industries Biomedical Engineering Co., Ltd., Shenzhen, China). For evaluation of systemic dyslipidemia, serum total cholesterol (TC), high-density lipoprotein cholesterol (HDL-C) and triglycerides (TG) were measured using a semi-automatic analyzer (Diatron Pictus B) with commercial reagent kits (Spinreact, Sant Esteve de Bas, Spain) according to the manufacturer's protocols. Low-density lipoprotein cholesterol (LDL-C) was calculated using the standard Friedewald equation [21]:

$$\text{LDL-C (g/L)} = TC - HDL\text{-}C - (TG/5)$$

2.5. A tissue assay of the hippocampus

2.5.1. Tissue Preparation

In this experiment, rats were randomly allocated to two groups: a control group (CON, n = 6) and a high-fat diet group (HFD, n = 6). Immediately after the blood was drawn, brains were rapidly excised, bisected, and the hippocampi were precisely dissected bilaterally on ice to preserve enzymatic integrity. Fresh hippocampal tissues were homogenized with ice-cold physiological saline (0.9% NaCl, w/v) at a ratio of 1:10 (w/v) using a Polytron homogenizer (T25 Ultra-Turrax; IKA-Werke, Staufen, Germany). The homogenates were centrifuged at 4 °C for 20 min at 10,000 × g. Supernatants were collected, divided into aliquots and stored at −20 °C. Total protein concentration was determined by Bradford method 22 using bovine serum albumin (BSA) as the standard.

2.5.2. Quantification of Transaminases and Inflammatory Markers

Key metabolic and inflammatory markers were measured. Hippocampal ALT; EC 2.6.1.2 and AST; EC 2.6.1.1 activities were evaluated spectrophotometrically as described by Bergmeyer

23. Enzyme activities are expressed as U/mg protein. To quantify neuroinflammation, IL-6 levels were analyzed utilizing a Chemiluminescence Immunoassay platform (MAGLUMI™ 800).

2.5.3. Assessment of Hippocampal Oxidative Stress Parameters

As the brain is particularly susceptible to lipotoxicity-induced ROS, an oxidative stress panel was performed on the hippocampal supernatants. All specific enzyme activities and concentrations were normalized to the total protein content:

Lipid Peroxidation (LPO): It was measured as malondialdehyde (MDA) equivalent by the thiobarbituric acid reactive substances (TBARS) assay at λ=532 nm [24]. Reduced Glutathione (GSH): Determined colorimetrically at 412 nm with Ellman's reagent (DTNB) [25,26]. Catalase (CAT, EC 1.11.1.6): Activity was measured by monitoring the kinetic decomposition of H 2 O 2 at 240 nm [27]. Glutathione Peroxidase (GPx, EC 1.11.1.9): Estimated by measuring the rate of GSH consumption at 412 nm according to the method of Flohé and Günzler [28]. Glutathione S-Transferase (GST, EC 2.5.1.18): (Measured by conjugation of 1-chloro-2,4-dinitrobenzene (CDNB) at 340 nm [29].

2.6. Histopathological analyses of the CA1 subfield

In this experiment, rats were randomly allocated to two groups: a control group (CON, n = 6) and a high-fat diet group (HFD, n = 6). To provide structural correlates for the observed biochemical and cognitive deficits, targeting the CA1 subfield heavily implicated in spatial memory, extracted brains were immersion-fixed in 10% neutral buffered formalin for 48 hours, dehydrated through a graded alcohol series, and embedded in paraffin. Coronal sections (5 μm thick) were generated using a rotary microtome.

Neuronal Morphometry: Sections were subjected to cresyl violet (Nissl) staining to microscopically assess cytoarchitecture, cellular density, and overt neurodegeneration within the pyramidal cell layer.

GFAP Immunohistochemistry: To visualize reactive astrogliosis, sections underwent heat-induced epitope retrieval (Tris-EDTA, pH 9.0) followed by the quenching of endogenous peroxidases (3% H_2O_2). Tissues were blocked with BSA and incubated with a primary anti-Glial Fibrillary Acidic Protein (GFAP) antibody (1:1000). Signal amplification was performed via an HRP-conjugated secondary antibody (1:100) and visualized using 3,3'-diaminobenzidine (DAB) chromogenesis. Sections were counterstained with toluidine blue prior to qualitative and quantitative analysis.

Imaging was conducted using a high-resolution light microscope (Max300; Premiere®) integrated with a digital camera (MA89, 5.0 megapixels) and Cam2 V5.4 capture software.

2.7. Statistical Analysis

Statistical analysis was conducted using SPSS version 20.0 (SPSS Inc., Chicago, IL, USA). All data are presented as mean ± standard error of the mean (SEM). To assess significant differences between two diet effects, the normality of variable distributions was tested using the Shapiro–Wilk test. A Student's T-test was then applied, and differences were considered statistically significant at $p<0.05$.

3. Results and Discussions

3.1. Effect of the HFD diet on weight gain

To evaluate the somatic effect of dietary intervention, the body weight gain after ten weeks of treatment was calculated (linking to Section 2.2). As shown in Table 1, rats fed with daily high-fat emulsion (HFD group) had a demonstrated increase in percentage of body weight gain (51.37 ± 0.84%) compared to standard diet control (CON) group (46.39 ± 1.06%) ($p = 0.0070$). This robust 4.98% divergence supports the efficacy of the emulsion-based delivery model in the successful induction of a systemic hyper-caloric phenotype prior to cognitive and biochemical testing Table 1.

3.2. HFD Impairs spatial working memory and Locomotor Activity

Spatial working memory and general exploratory behavior were measured using the Y-maze spontaneous alternation test (Figure 1). After 10 weeks of dietary intervention, the HFD group displayed a significantly lower percentage of spontaneous alternation (65.00 ± 1.91%) compared with CON rats (70.14 ± 1.03%) ($p = 0.0234$), indicating a deficit in hippocampus-dependent working memory. At the same time, the locomotor and exploratory activity were significantly reduced in the HFD cohort, as demonstrated by the decreased total arm entries (20.57 ± 1.13) when compared with the CON group (28.00 ± 0.90) ($p = 0.0040$).

3.3. Alterations in Systemic Glycemic and Lipid Profiles

To characterize the peripheral metabolic foundation preceding CNS alterations (Section 2.4.1), fasting glycemic and lipid profiles were quantified (Table 2). The 10-week HFD regimen induced significant

systemic dyslipidemia, marked by elevated serum TG (1.533 ± 0.084 g/L vs. 1.196 ± 0.082 g/L, p = 0.0111), TC (1.746 ± 0.115 g/L vs. 1.289 ± 0.067 g/L, p = 0.0059), and LDL (1.147 ± 0.081 g/L vs. 0.947 ± 0.029 g/L, p = 0.0099) compared to CON animals. HDL levels demonstrated a non-significant trend toward reduction (p = 0.0960). Interestingly, fasting blood glucose and serum insulin levels remained statistically unaltered (p = 0.0880 and p = 0.0630, respectively), indicating that the observed metabolic disturbance at this temporal stage is predominantly lipid driven.

Table 1. *Effect of a 10-week HFD on body weight gain (%) in male Wistar rats*

Parameter	CON (n=12)	HFD (n=12)	P-value	Significance
weight gain (WG) (%)	46.39 ± 1.06	51.37 ± 0.84	0.0070	**

Data are expressed as mean ± standard deviation (SEM). Difference is very significant (**P < 0.01), compared with CON group.

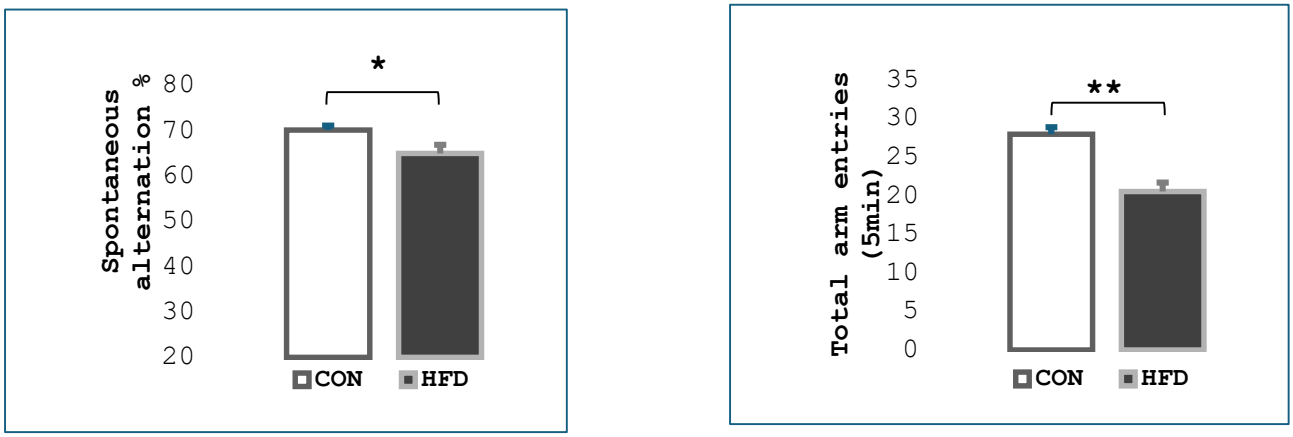

Figure 1. *HFD impairs spatial working memory and exploratory behavior in the Y-maze test. (A) Percentage of spontaneous alternation performance. (B) Total number of arm entries recorded over a 5-minute exploratory perio*d. *Data are expressed as mean ± standard deviation (SEM); (n = 12).Difference is significant (* p ≤ 0,05), (**p ≤ 0,01) very significant, compared with CON group.*

Table 2. Impact of a 10-week HFD on systemic glycemic and lipid profiles.

Parameter	CON (n=12)	HFD (n=12)	P-value	Significance
Blood glucose (mg/dL)	95.55 ± 1.44	98.47 ± 1.06	0.088	NS
Serum Insulin Levels (mU/L)	74.33 ± 0.89	76.55 ± 0.52	0.0630	NS
TG (g/L)	1.196 ± 0.082	1.533 ± 0.084	0.0111	*
TC (g/L)	1.289 ± 0.067	1.746 ± 0.115	0.0059	**
HDL (g/L)	0.5743 ± 0.050	0.4571 ± 0.0377	0.0960	NS
LDL (g/L)	0.9471 ± 0.029	1.147 ± 0.081	0.0099	**

Data are expressed as mean ± standard deviation (SEM). Difference is Not Significant (NS), significant (* p ≤ 0,05), (**p ≤ 0,01) very significant, compared with CON group.

3.4. HFD Increases Hippocampal Transaminase Activity and Neuroinflammation

Transaminase activity and pro-inflammatory signaling in hippocampal homogenates were assessed to determine the translation of peripheral metabolic dysfunction into CNS distress (Table 3). HFD administration resulted in a near-doubling of hippocampal ALT activity (9.66 ± 1.36 IU/mg protein) compared to controls

Table 3. *Effects of a 10-week HFD on hippocampal transaminase activity and IL-6 levels.*

Parameter	CON (n=6)	HFD (n=6f)	P-value	Significance
ALT (IU/mg protein)	4.91 ± 1.01	9.66 ± 1.36	0.0171	*
AST (IU/mg protein)	2.59 ± 1.87	7.59 ± 1.02	0.0427	*
IL-6 (pg/mg protein)	9.58 ± 1.36	17.63 ± 2.36	0.0150	*

Data are expressed as mean ± standard deviation (SEM). Difference is significant (* p ≤ 0,05), compared with CON group.

3.5. HFD Induces Hippocampal Oxidative Stress and Impairs Antioxidant Defenses

To evaluate the hippocampal oxidative status, a complete panel of pro-oxidant and antioxidant biomarkers (Table 4) was used. HFD exposure caused a pronounced oxidative imbalance, evidenced by an almost twofold increase in malondialdehyde (MDA) levels, a major marker of lipid peroxidation (LPO), in the HFD group (22.39 ± 3.08 nmol/mg protein) compared with the CON group (11.65 ± 2.98 nmol/mg protein, p = 0.0276).The activity of AST was also significantly increased in the HFD group (7.59 ± 1.02 IU/mg protein vs. 2.59 ± 1.87 IU/mg protein, p = 0.0427). Simultaneously, the level of pro-inflammatory cytokine IL-6 was significantly elevated by 84% in HFD-fed rats (17.63 ± 2.36 pg/mg protein) compared to CON rats (9.58 ± 1.36 pg/mg protein) (p = 0.0150), confirming active neuroinflammation.

Table 4. *Effects of a 10-week HFD on hippocampal oxidative stress and antioxidant defense parameters.*

Parameter	CON (n=6)	HFD (n=6)	P-value	Significance
LPO (MDA) (nmol/mg protein)	11.65 ± 2.98	22.39 ± 3.08	0.0276	*
GSH (nmol/mg protein)	16.35 ± 1.89	7.98 ± 2.21	0.0142	*
GPx (nmol GSH/mg protein)	6.39 ± 1.08	2.36 ± 0.98	0.0173	*
GST (nmol CDNB/min/mg protein)	52.36 ± 5.98	29.36 ± 6.36	0.0218	*
CAT (µmol H_2O_2/min/mg protein)	160.84 ± 8.35	118.69 ± 9.36	0.0058	**

Data are expressed as mean ± standard deviation (SEM). Difference is significant (* $p \leq 0,05$), (** $p \leq 0,01$) very significant, compared with CON group.

3.6. HFD Alters Neuronal Morphology in the Hippocampal CA1 Subfield

To determine the structural consequences of lipotoxic injury, neuronal morphology within the CA1 subfield was assessed using Nissl (cresyl violet) staining (Figure 2). In the CON group, the CA1 pyramidal cell layer exhibited regular cytoarchitecture with structurally organized, healthy neurons (NN) featuring distinct nuclei and nucleoli, alongside physiological glial density (Figure 2A, C). Conversely, the hippocampi of HFD-fed rats showed marked structural disorganization. The CA1 pyramidal layer of the HFD group revealed widespread signs of neuronal distress, characterized by neuronal atrophy (AN), cytoplasmic shrinkage, and nuclear pyknosis (Figure2: B, D). Qualitative observation of these sections also revealed a prominent increase in the population density of surrounding glial cells (A, M, O) in response to dietary insults figure 2.

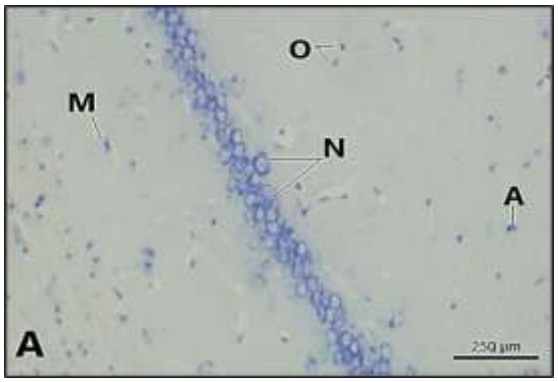

3.7. HFD Induces Astrogliosis and GFAP Upregulation in Hippocampus

To confirm the increase of biochemical inflammatory markers, astrocytic reactivity was evaluated by immunohistochemistry for Glial Fibrillary Acidic Protein (GFAP) in the CA1 region (Figure 3). Control animals showed moderate, localized GFAP expression consistent with a physiological "surveillance" state with typical ramified astrocytic arborization in the pyramidal and molecular layers (Figure 3A, C). In contrast, HFD treated animals showed diffuse and enhanced GFAP immunoreactivity. Astrocytes in the HFD cohort demonstrated typical morphological hallmarks of reactive astrogliosis, including cellular hypertrophy, increased cell body size, and prominent structural processes that were confluent (Figure3: B, D). This visual evidence is definitive and corresponds to increased IL-6 levels, suggesting strong diet-induced neuroinflammation figure 3.

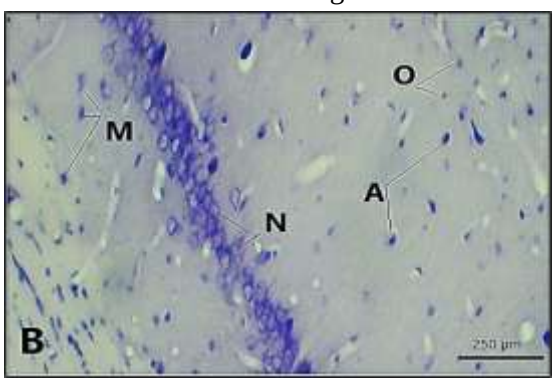

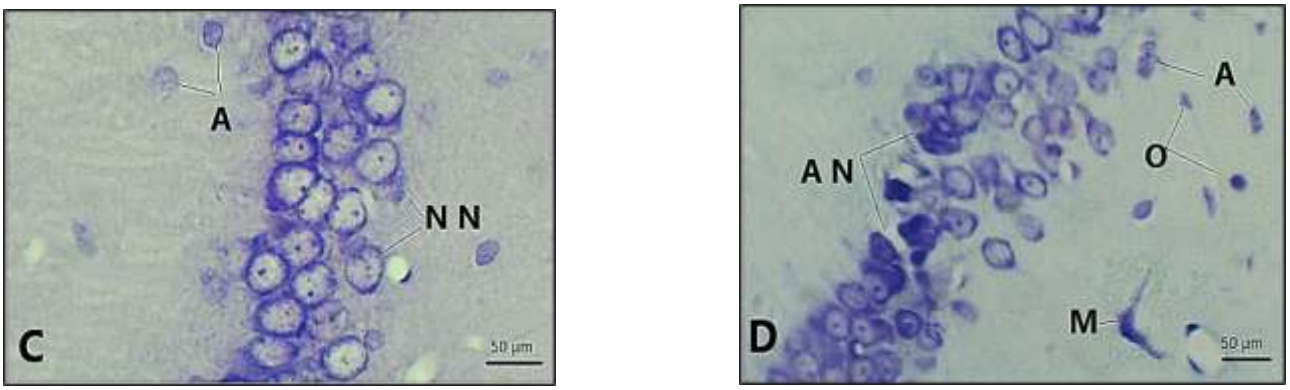

Figure 2. *Histopathological changes in in the hippocampal CA1 region of HFD after 10 weeks of dietary intervention. Representative photomicrographs of cresyl violet (Nissl) staining in CON (A, C) and HFD (B, D) rats. (A, B) Show the pyramidal cell layer architecture. (100). (C, D) Illustrate the details of the CA1 areas (400×). The CON exhibits normal neuronal morphology (NN). The HFD group displays affected/pyknotic neurons (AN). A: Astrocytes, M: microglia (M) and O: oligodendrocytes.*

Histopathological changes in in the hippocampal CA1 region after 10 weeks of dietary intervention. Representative photomicrographs of cresyl violet (Nissl) staining in CON (A, C) and HFD (B, D) rats. (A, B) Show the pyramidal cell layer architecture. (100). (C, D) Illustrate the details of the CA1 areas (400×). The CON exhibits normal neuronal morphology (NN). The HFD group displays affected/pyknotic neurons (AN). A: Astrocytes, M: microglia (M) and O: oligodendrocytes.

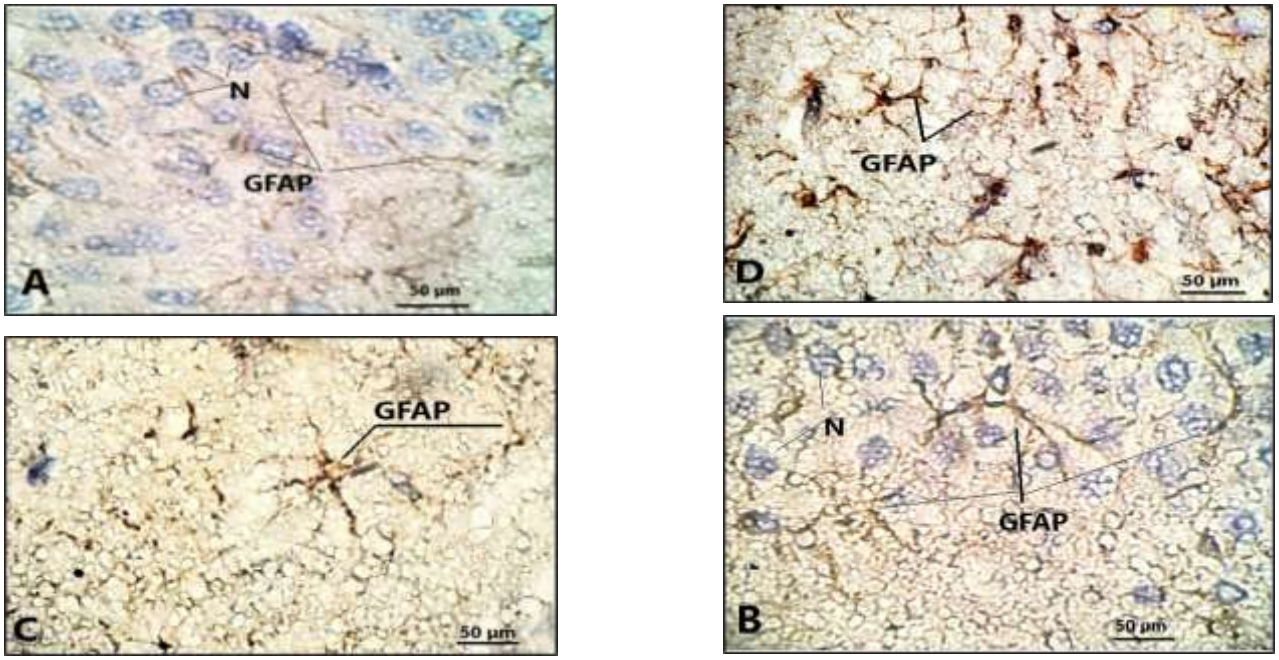

Figure 3. *Immunostaining for GFAP in the hippocampal CA1 region following 10 weeks of dietary intervention. Representative photomicrographs of the pyramidal cell layer (A, B) and molecular layer (C, D) (400×). The CON group (A, C) presents normal astrocyte morphology in resting condition. (B, D) In the HFD group, there is increased GFAP, suggestive of reactive astrogliosis. Sections were counterstained with toluidine blue. N: Neuron.*

4. Discussion

The present study shows that 10 weeks of HFD emulsion initiates a cascade of pathological events beginning from systemic dyslipidemia towards hippocampal neurodegeneration and spatial memory deficits. The average weight gain observed was consistent with well-established models of diet-induced obesity [30,31]. Interestingly, the emulsion-based delivery system by gavage allowed for controlled delivery of nutrients, resulting in the effective induction of an obesity phenotype at a faster rate than traditional pellet-based models [15,32]. Behaviorally, HFD exposure induced significant deficits in spatial working memory, reflected in significant decreases in Y-maze

spontaneous alternation and exploratory behavior. In contrast to previous work, which frequently emphasizes cognitive decline after long-term (12-16 weeks) HFD exposure [2,33,34], our findings show that 10 weeks is enough to severely impair hippocampal-dependent navigation and memory consolidation. Such rapid cognitive decline is intrinsically related to the peripheral metabolic disturbances observed in our model.

Metabolically, HFD animals exhibited systemic dyslipidemia (increased TC, LDL, and TG) without significant changes in fasting blood glucose or insulin. This profile is of clinical relevance as it isolates lipotoxicity rather than glucotoxicity or overt diabetes as the primary peripheral trigger for subsequent CNS pathologies [1,5]. Circulating lipid perturbagens disrupts the BBB integrity, allowing peripheral lipid and inflammatory signal entry into the brain parenchyma [35,36, 37].

The overload of lipids in hippocampus impairs the local metabolic homeostasis [38,39]. This was clearly translated by the significant increase of hippocampal ALT and AST transaminases. Brain transaminases are important for the malate-aspartate shuttle and glutamate-glutamine cycling [16,17,18], but are usually assessed as hepatic markers. Their elevation is indicative of severe mitochondrial stress and compensatory but ultimately damaging shifts in cellular energy production in response to lipid influx [16,17,18].

Such mitochondrial dysfunction will inevitably lead to the overproduction of ROS. Our biochemical assays showed the drastic collapse of the antioxidant defense system of the hippocampus, characterized by decreased GSH levels and reduced activity of GPx, GST, and CAT. Thus, the levels of lipid peroxidation (MDA) were almost doubled. The brain is particularly vulnerable to such oxidative insults due to its high oxygen demand and dense polyunsaturated lipid matrix [3,4]. This oxidative stress synergizes with neuroinflammation. ROS and lipid peroxides are danger-associated molecular patterns (DAMPs) that activate glial cells [6,7,8,9]. The dramatic 84% increase in hippocampal IL-6 we observed in our study is strong biochemical evidence of this pro-inflammatory response, establishing a direct link between lipotoxicity and cytokine release.

The biochemical toxicity was reflected in clear structural damage to the CA1 region, a critical center for spatial memory. Histopathological analysis (Fig. 2) showed significant neuronal distress with pyknotic nuclei and cytoplasmic shrinkage in the HFD group, indicative of early-stage neurodegeneration [13,40]. Concomitant GFAP immunohistochemistry showed extensive astrogliosis. Animals treated with HFD showed severe hypertrophy of astrocytes with respect to the physiological ramified state observed in controls. Reactive astrocytes frequently exhibit downregulation of essential glutamate transporters (e.g., GLT-1/EAAT2), which results in reduced synaptic glutamate clearance and subsequent excitotoxicity [41,42,43]. This synaptic homeostasis disruption, as a consequence of the vicious cycle of oxidative stress and glial inflammation [10,11], provides the structural and mechanistic explanation for the spatial memory deficits observed in the Y-maze.

5. Conclusion

This study shows that short-term HFD for 10 weeks is sufficient to significantly impair spatial working memory by lipotoxicity-driven mechanism and not hyperglycemia. Systemic dyslipidemia induces a cascade of central disturbances in the hippocampus by changes in transaminases activity, high oxidative stress and failure of antioxidant defenses. At the structural level, astrogliosis increased neuroinflammation in the form of IL-6, and neuronal degeneration in the CA1 subfield reflects these biochemical changes. Together, these findings demonstrate the extreme vulnerability of the hippocampus to dietary lipid excess and underscore the critical importance of the peripheral-central metabolic axis in the early development of diet-induced cognitive decline.

Author Statements:

- **Ethical approval:** The conducted research is not related to either human or animal use.
- **Conflict of interest:** The authors declare that they have no known competing financial interests or personal relationships that could have appeared to influence the work reported in this paper
- **Acknowledgement:** The authors declare that they have nobody or no-company to acknowledge.

References

[1] Kullmann, S. Kleinridders, A. Small D.M, Fritsche, A. Harin H.U, Preissl H. Heni M. (2020). Central nervous pathways of insulin action in the control of metabolism and food intake. *Lancet Diabetes Endocrinol.* (6): 524–534.

[2] Mackey-Alfonso, S. E and Barrientos, R. M. (2025). Neuroinflammatory mechanisms linking high-fat diets to Alzheimer's disease

vulnerability: Beyond the amyloid hypothesis. *Alzheimers Dement*. 21: e70911.

[3] Cobley, J. N. Fiorello, M. L. & Bailey D. M. (2018). 13 reasons why the brain is susceptible to oxidative stress. *Redox Biology*. 15: 490-503.

[4] Díaz, M. Valdés-Baizabal, C. de Pablo, DP. Marin, R. (2024). Age-dependent changes in Nrf2/Keap1 and target antioxidant protein expression correlate to lipoxidative adducts and are modulated by dietary N-3 LCPUFA in the hippocampus of mice. *Antioxidants Basel*. 13:2.

[5] de Paula, GC. Brunetta, HS. Engel, DF. Gaspar, JM. Velloso LA. Engblom D. (2021). Hippocampal function is impaired by a short-term High-Fat Diet in mice: increased blood-brain barrier permeability and Neuroinflammation as triggering events. *Front Neurosci-Switz*. 15 :734158.

[6] Teleanu, D. M. Niculescu, A. G, Lungu, I.I, Radu C.I, Vladâcenco O. Roza E. Costăchescu B. Grumezescu A. M, Teleanu R. I. (2022). An Overview of Oxidative Stress, Neuroinflammation, and neurodegenerative diseases. *Int. J. Mol. Sci*. 23: 5938.

[7] Dmytriv, T. Duve, K. Lushchak V. (2024). Vicious cycle of oxidative stress and neuroinflammation in pathophysiology of chronic vascular encephalopathy. *Front. Physiol.* 15:1443604.

[8] Chun H. H, Kang Y. Kim Y. Shin J. (2020). Severe reactive astrocytes precipitate pathological hallmarks of Alzheimer's disease via H2O2 production. *Nat. Neurosci*. 23:1555–66.

[9] Escartin, C. Galea E. Lakatos, A. O'Callaghan J. Petzold G. (2021). Reactive astrocyte nomenclature, definitions, and future directions. *Nat. Neurosci*. 24:312–25.

[10] Yang, G. Xu, X. Gao, W. Wang, X. Zhao, Y. Xu Y. (2025). Microglia-Orchestrated Neuroinflammation and Synaptic Remodeling: Roles of pro-Inflammatory Cytokines and Receptors Neurodegeneration. *Front. Cell. Neurosci*. 19:1700692.

[11] Srokowska, M. Zwierello, W. Wszolek, A. Gutowska I. (2025). Neurobiochemical Effects of a High-Fat Diet: Implications for the Pathogenesis of Neurodegenerative *Diseases. Biology*. 14: 1317.

[12] Gao, Q.L, Zha, H., Liu, Z.J. (2025). Hippocampal CA1 neuron, a crucial regulator for chronic stress exacerbating alzheimer's disease progression. *Cell Biosci.* 15:73.

[13] Teng, S.F, Lee, M.T, Lee, L.J, Hwang, L.L, Chen, C.P, Lee H.J, Chen, C.T, Chiou L.C. (2025). High-fat diet impairs the dendritic morphology of hippocampal CA1 pyramidal neurons in male but not female mice. *Front Nutr*. 12:1687060.

[14] Arnold, S.E, Lucki, I, Brookshire, B.R et al. (2014). High fat diet produces brain insulin resistance, synaptodendritic abnormalities and altered behaviour in mice. *Neurobiol Dis*. 67:79–87.

[15] Mostafa, M.D, Amer, M.E, ElKomy, M.A, Othman, A.I, El-Missiry, M.A. (2025). controlled obesity and invigorated cognitive and memory performance in rats consuming a high-fat diet via modulating oxidative stress, inflammation and apoptosis. *Sci Rep*. 15(1): 20171.

[16] Singh, T, Kwatra, M, Kushwah, P, Pant, R, Bezbaruah B.K. (2022). Jangra Binge alcohol consumption exacerbates high-fat diet-induced neurobehavioral anomalies: possible underlying mechanisms Chem. *Biol. Interact*. 364: 110039.

[17] Custodio, R.J, Hobloss, P. Z, and Myllys, M. (2023). Cognitive Functions, Neurotransmitter Alterations, and Hippocampal Microstructural Changes in Mice Caused by Feeding on Western Diet. *Cells.* 12(18).

[18] Treviño, S, Díaz, A, González-López, G, Guevara, J. (2022). Differential biochemical-inflammatory patterns in the astrocyte-neuron axis of the hippocampus and frontal cortex in wistar rats with metabolic syndrome induced by high fat or carbohydrate diets. *J Chem Neuroanat*. 126: 102186.

[19] Deacon, R.M, Rawlins, J.N. (2006). T-maze alternation in the rodent. *Nature Protocols*. 1(1) :7–12.

[20] Swonger, A, and Rech, R. (1972). Serotonergic and cholinergic involvement in habituation of activity and spontaneous alternation of rats in a Y maze. *J Comp Psychol.* 81: 509–522.

[21] Friedewald, W, Levy, R, Fredrickson, D. (1972). Estimation of the concentration of low-density lipoprotein cholesterol in plasma, without use of the preparative ultracentrifuge. *Clin Chem*. 18: 499-502.

[22] Bradford, M. M. (1976). A rapid and sensitive method for the quantitation of microgram quantities of protein utilizing the principle of protein-dye binding. *Analytical Biochemistry*. 72(1-2): 248-254.

[23] Bergmeyer, H. U, Scheibe, P, & Wahlefeld, A. W. (1978). Optimization of methods for aspartate aminotransferase and alanine aminotransferase. *Clinical Chemistry*. 24(1): 58-73.

[24] Buege, J. A, & Aust, S. D. (1984). Microsomal lipid peroxidation. Methods in *Enzymology*. 105: 302-10.

[25] Ellman, G. L. (1959). Tissue sulfhydryl groups. *Archives of Biochemistry and Biophysics*. 82(1): 70-7.

[26] Jollow, D. J, Mitchell, J. R, Zampaglione, N, & Gillette, J. R. (1974). Bromobenzene-induced liver necrosis. Protective role of glutathione and evidence for 3, bromobenzene oxide as the hepatotoxic metabolite. *Pharmacology*. 11(3): 151-69.

[27] Aebi, H. (1984). Catalase in vitro. Methods in *Enzymology*. 105: 121-6.

[28] Flohe, L, Gunzler, W.A. (1984). Analysis of glutathione peroxidase. *Methods in Enzymology*. 105: 114-21.

[29] Habig, W.H, Pabst, M.J, & Jakoby, W.B. (1974). Glutathione- Stransferase the first step in mercapturic acid formation. *Journal of Biological Chemistry.* 249(22): 7130-9.

[30] Marques, C, Meireles, M, Norberto, S, Leite, J, Freitas, J, Pestana, D, Faria, A, Calhau, C. (2015). High-fat diet-induced obesity rat model: a comparison between Wistar and Sprague-Dawley rat. *Adipocyte*. 5(1):11–21.

[31] Sanguinetti, E, Guzzardi, M.A, Panetta, D, Tripodi, M, De Sena, V, Quaglierini, M, et al. (2019). Combined Effect of Fatty Diet and Cognitive Decline on Brain Metabolism, Food Intake, Body Weight, and Counteraction by Intranasal Insulin Therapy in 3xTg Mice. *Front Cell Neurosci.* 13:188.

[32] Zou, Y, Li J, Lu, C, Wan,g J, Ge J, Huang, Y, Zhang, L, Wang, Y. (2006). High-fat emulsion-induced rat model of nonalcoholic steatohepatitis. *Life Sci*. 79:1100–1107.

[33] Ribeiro, R, Silva, E. G, Moreira, F. C, Gomes, G. F, Cussat, G. R, Silva, B. S. R, da Silva, M. et al. (2023). Chronic hyperpalatable diet induces impairment of hippocampal-dependent memories and alters glutamatergic and fractalkine axis signaling. *Scientific Reports*. 13(1): 16358.

[34] Butler, M.J, Muscat, S.M, Caetano-Silva M.E, Shrestha, A, Olmo B.M.G, Mackey-Alfonso S.E, Massa N, Alvarez B.D, Blackwell J.A, Bettes M.N, et al. (2025). Obesity-associated memory impairment and neuroinflammation precede widespread peripheral perturbations in aged rats. *Immun. Ageing*. 22: 2.

[35] Rhea, E.M, Banks, W.A. (2021). Interactions of Lipids, Lipoproteins, and Apolipoproteins with the Blood-Brain Barrier. *Pharm. Res*. 38: 1469–1475.

[36] Hsu, T.M, Kanoski, S.E. (2014). Blood-Brain Barrier Disruption: Mechanistic Links between Western Diet Consumption and Dementia. *Front. Aging Neurosci*. 6: 88.

[37] Leidmaa, E, Zimmer, A, Stein, V, Gellner, A.-K. (2025). Acute High-Fat High-Sugar Diet Rapidly Increases Blood–Brain Barrier Permeability in Mice. *J. Nutr. Health Aging.* 29: 100574.

[38] Berghoff, S.A, Spieth, L, and Saher, G. (2022). Local cholesterol metabolism orchestrates remyelination. *Trends Neurosci*. 45: 272–283.

[39] Vanherle, S, Loix, M, Miron, V.E, Hendriks, J.J.A, and Bogie, J.F.J. (2025). Lipid metabolism, remodelling and intercellular transfer in the CNS. *Nat. Rev. Neurosci*. 26: 214–231.

[40] Alkan, I, Altunkaynak, B. Z, Gültekin, G. İ & Bayçu, C. (2021). Hippocampal neural cell loss in high-fat diet-induced obese rats-exploring the protein networks, ultrastructure, biochemical and bioinformatical markers. *J. Chem. Neuroanat.* 114: 101947.

[41] Mota, B, Brás, A.R, Araújo-Andrade, L, Silva, A, Pereira, P.A, Madeira, M.D, Cardoso, A. (2024). High-Caloric Diets in Adolescence Impair Specific GABAergic Subpopulations, Neurogenesis, and Alter Astrocyte Morphology. Int. *J. Mol. Sci*. 25: 5524.

[42] Pajarillo E, Rizor A, Lee J, Aschner M, Lee E. (2019). The role of astrocytic glutamate transporters GLT-1 and GLAST in neurological disorders: Potential targets for neurotherapeutics. *Neuropharmacology.* 161: 107559.

[43] Tsai, S.F, Hsu, P.L, Chen, Y.W, Hossain M.S, Chen, P.C, Tzeng, S.F, Chen, P.S, Kuo, Y.M. (2022). High-fat diet induces depression-like phenotype via astrocyte-mediated hyperactivation of ventral hippocampal glutamatergic afferents to the nucleus accumbens. *Mol. Psychiatry*. 27: 4372–4384.